Polymer Chemistry

Mechanochromic Composite Elastomers for Additive Manufacturing and Low Strain Mechanophore Activation

Journal:	*Polymer Chemistry*
Manuscript ID	PY-ART-07-2019-001053.R1
Article Type:	Paper
Date Submitted by the Author:	02-Sep-2019
Complete List of Authors:	Rohde, Rachel; University of California Berkeley, Chemistry Basu, Amrita; University of Washington, Chemistry Okello, Lilian; North Carolina State University, Chemical and Biomolecular Engineering Barbee, Meredith; Duke University, Chemistry Velev, Orlin; North Carolina State Univ., Chemical Biomolecular Engineering Nelson, Alshakim; University of Washington, Chemistry Craig, Stephen; Duke University, Department of Chemistry

ARTICLE

Mechanochromic Composite Elastomers for Additive Manufacturing and Low Strain Mechanophore Activation

Received 00th January 20xx,
Accepted 00th January 20xx

DOI: 10.1039/x0xx00000x

Rachel Rohde,[a] Amrita Basu,[b] Lillian B. Okello,[c] Meredith H. Barbee,[a] Orlin D. Velev,[c,*] Alshakim Nelson,[b,*] Stephen L. Craig[a,*]

Herein, we report a strategy for additive manufacturing of a mechanochemically active silicone ink primarily comprised of PDMS microbeads. Extruded, stable structures of cured microbeads were held together with a "bridging material" comprising uncured PDMS and spiropyran in a water medium. The mechanochromic silicone ink was a shear-thinning gel that exhibited a yield stress, and thus, was suitable for direct-write 3D printing. The spiropyran was stable to mild conditions of the printing process, and after a thermal curing step, the printed silicone displayed reversible mechanochromic activity. The extruded composite displays chromophore activation at lower mechanical strains under uniaxial tension (60-70%) than in a film without the microbeads (130-140%). Multi-layered 3D printed constructs were fabricated and displayed mechanochromic activity in tension and compression. These experiments demonstrate the versatility of these silicone inks to produce 3D printed functional elastomers with mechanochemical activity.

Introduction

Three-dimensional printing (3DP) has gained prominence in the last decade as an effective, low-cost method of prototyping for a variety of applications.[1] Recently, the merger of commercially available 3DP technologies and increasingly functional polymeric filaments have given rise to promising potential 3DP applications including bioprinting tissues and organs,[2,3] drug-delivery,[4] and materials for energy storage.[5] Material extrusion remains among the most widely used 3DP techniques and can be used to print materials ranging from thermoplastics to metals.[6,7] The extrusion-based direct writing of elastomeric materials, however, remains challenging as their precursors are usually liquids under ambient conditions and their viscoelastic properties are not suitable for building multi-layered constructs. Silicones, for example, are of interest for 3DP applications as they have favorable elastomeric properties and optical clarity, but there are few examples of silicone precursors that are suitable for direct-write 3DP.[8–10] Recently, Roh and coworkers reported that a dispersion of PDMS microbeads in a secondary PDMS matrix that offers a promising strategy for 3DP of PDMS.[11] The "ink" comprises a high ratio of cured PDMS microbeads to uncured PDMS precursor, which is dispersed in water to form a thixotropic granular paste that can be extruded into discrete objects.[11] The structures reported are mechanically stable owing to the formation of inter-bead capillary bridges formed by the uncured PDMS in the presence of water; similar forces are responsible for the creation and stability of sand castles. This "homocomposite" paste[8] has a high storage modulus and yield stress that allow it to be extruded at room temperature with an adapted 3D printer. The resulting structures are highly elastic, and the process can produce intricate meshes and other structures.[11,12]

Recent interest in stimuli responsive materials to be used in 3DP has spurred the design of innovative molecular functionalities:[13] including shape-memory polymers,[14–16] electroluminescent materials[17] and materials with functional molecular recognition.[18–20] Mechanically-responsive materials, such as those based on covalent mechanophores, remain relatively unexplored for use in 3DP.[21,22] In mechanophore-based polymers, the strain felt in a polymer network changes the chemical potential energy of a desired chemical reaction. Historically, this reactivity was limited to homolytic bond scission reactions and the weakening of the polymeric material,[23,24] but the past decade has seen mechanophores used to drive responses that include self-strengthening,[25] chemical cargo release,[26] mechanochromism[27] and luminescence.[28] Spiropyran derivatives (SP) are among the most widely studied mechanophores and have been incorporated into commercial silicones to undergo a strain induced ring-opening reaction to yield a conjugated, colored merocyanine (MC)[29] (Fig. 1-a). If the mechanophore is appropriately embedded in the polymer network so that isomerization is coupled to the molecular-level tension in the network, the strain in the network can be monitored visually. The SP to MC reaction is reversible and repeatable; the color disappears when

[a] Department of Chemistry, Duke University, Durham, NC 27708 stephen.craig@duke.edu.
[b] Department of Chemistry, University of Washington, Seattle, WA 98112 alshakim@uw.edu
[c] Department of Chemical and Biomolecular Engineering, North Carolina State University, Raleigh, NC 27695 odvelev@ncsu.edu

Electronic Supplementary Information (ESI) available: [details of any supplementary information available should be included here]. See DOI: 10.1039/x0xx00000x

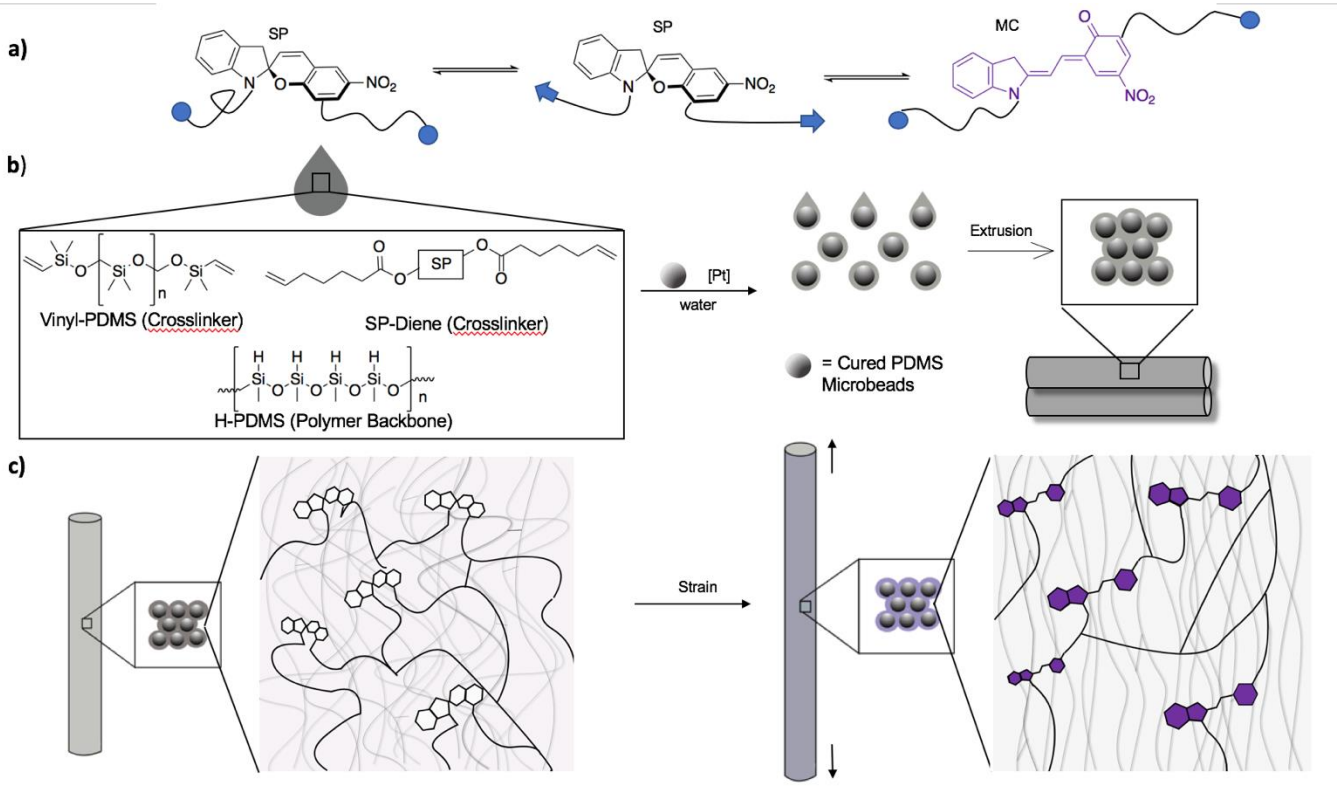

Fig. 1: a) (Left to right) SP is covalently incorporated into the polymer network. Macroscopic strain is transferred to the SP via the polymer network, resulting in enthalpic distortions to SP. At a critical force, SP isomerizes to MC and dissipates the force experienced by the polymer network. **b)** The SP-diene is incorporated with Dragon Skin 30 vinyl-PDMS crosslinkers, H-PDMS and platinum catalyst. Cured Sylgard™ 184 microbeads are suspended in Dragon Skin 30 with incorporated SP. The resulting thixotropic paste is formed in the presence of water due to capillary action and is extruded and cured overnight at 80 °C. **(c)** Cured, extruded material at 0% strain with ring-closed SP crosslinked into the polymer network. After the material experiences strain, the composite displays mechanochromic activity at the bridging sites due to strain-induced ring-opening of spiropyran to form MC.

the material relaxes and returns if the elastomer is strained again.

There have been relatively few examples of 3D printable mechanoresponsive materials, perhaps because many mechanophores can undergo irreversible reactions under printing conditions.[30] Recently, Boydston and coworkers reported printing poly(ε-caprolactone) (PCL) containing SP by filamentizing the polymers and printing structures with a commercially available fused deposition modelling (FDM) printer.[21] PCL was selected due to its relatively low melting point (~60 °C) and glass transition temperature, which allowed for milder printing conditions over other polymer systems; however, mechanochromic activation of the printed object only occurs as the object is irreversibly deformed. Boydston and coworkers also reported photopolymerizing complex object geometries containing an oxanorbornadiene based mechanophore that releases a small molecule.[22] The molecule was extracted and quantified with GC-MS to determine percent activation of mechanophore as a function of strain. While the objects display full shape recovery, the mechanochemical reaction is irreversible and cannot be visualized. To address these limitations, we set out to combine the silicone-based 3DP strategy reported by Roh and coworkers[11] with silicones with mechanochromic crosslinkers similar to those reported previously by Gossweiler et al.[31] Additionally, by incorporating SP into the uncured PDMS "bridging" material, we anticipated that the mechanophore would be concentrated at the interfaces between the beads where theoretical models predict stress to be concentrated under deformation,[32,33] via a mechanism that is reminiscent of the selective mechanochemical activation of a Diels-Alder adduct-based mechanophore at silica-polymer interfaces.[34] Therefore, we hypothesized that this printing platform would provide both a strategy to 3D print mechanophores in silicone materials that have increased mechanochromic activity compared to their bulk elastomer counterparts.

Experimental

Materials and Methods

Silicone Pre-Elastomers. Sylgard™ 184 base and Sylgard™ 184 crosslinking reagent (Dow Corning) was purchased from Ellesworth Adhesive, Germantown WI, Mowiol 18-88, xylene and Polysorbate 20 were purchased from Sigma-Aldrich. Dragon Skin™ A and B were purchased from Smooth-On. All silicone pre-elastomers and solvents were used as received without further purification.

Creating the PDMS Inks. The preparation of the PDMS ink first required the formation of PDMS microbeads. Sylgard™ 184

base and Sylgard™ 184 crosslinking reagent were combined in a 10:1 ratio. The PDMS prepolymer mixture was then vortexed for 5 min and promptly degassed on a vacuum manifold for 30 min. Then, 6 mL of the PDMS pre-polymer mixture and 250 mL of a 14 wt% aqueous solution of polyvinyl alcohol (Mowiol 18-88) were combined and vigorously stirred for 10 min using an overhead mechanical stirrer at 1000 rpm (OS40-Pro, SciLogex). The reaction was left to continue overnight at 80°C to afford cured PDMS microbeads. The beads were washed ten times with 50 mL of polysorbate 20 solution (0.1 wt%). Storage of the PDMS microbeads in polysorbate 20 solution (0.1 wt%) as 50 wt% suspensions was necessary to prevent aggregation. Bead diameters were in a range of 10-40 μm, as determined by analysis of SEM images.

The PDMS microbead was transformed into a gel via the formation of capillary bridges. A solution of SP dissolved in xylenes (175 mg/mL) was added to Dragon Skin™ 30 Part B. This solution was thoroughly mixed before an equal mass of Dragon Skin 30 Part A was added to yield a polymer comprised of 1:1 (Part A: Part B) and loaded with 0.5 wt% SP. The PDMS microbead suspension and uncured Dragon Skin 30 precursor with SP were combined and vortexed to achieve a final ink composition of 50 wt% of Dragon Skin 30 precursor, 50 wt% Sylgard™ 184 microbeads and 0.25 wt% SP. After 5 min, a visible sol-gel transition was observed. The gel was further mixed with a mortar and pestle. The final ink contains small amounts of water.

Extrusion and Curing of PDMS Inks. The silicone inks were hand loaded in a syringe and extruded by hand for preliminary characterization. The resulting structures were cured overnight at 85°C.

Characterizing Mechanochromic Composite Materials. The inks were imaged via variable pressure scanning electron microscopy (XL30 ESEM, FEI). Cursory images of the cured structures under manually administered tension and compression were taken with a digital microscope (AM3111, Dino-Lite). Tensile tests were performed on cylindrical samples of hand-extruded PDMS composite material with 0.25 wt% SP and Dragon Skin 30 thin films with 0.25 wt% SP and thin film samples of Dragon Skin 30 with 0.25 wt% SP. Samples were placed in a micro-strain analyzer (RSA IIIm TA Instruments) and the gap distance was subsequently set to zero the pressure reading. The gap speed was set to 1 mm s^{-1}. The tensile test was captured an SLR camera (Canon EOS RebelTM Xsi with a Canon EF-S 18-55 mm f/3.5-5.6 IS SLR lens). Images were white balanced by a color-neutral target card (OptekaTM Digital Color & White Balance Card), which was placed next to the instrument. The image was split into three color channels (red, green and blue) and the pixel intensity was quantified using Fiji ImageJ. The ratio of mean pixel intensity of the blue channel over the green channel was used to determine activation.

Rheological characterization of the PDMS ink. Rheological characterization of the uncured ink was performed on a TA Instrument DHR-2 rheometer fitted with a 20 mm parallel plate geometry with a gap of 1 mm. Each experiment was run with freshly prepared samples in order to avoid any extent of curing within the silicones. All samples were subject to oscillatory pre-shearing at 10 rad s^{-1} for 8 min to improve the reproducibility of the data. An oscillatory stress sweep was performed by subjecting the sample to a strain from 0.01% to 100% (1 Hz) to characterize the linear viscoelastic region of the material. A viscosity versus shear rate experiment was performed at 25 °C from 0.01 to 100 s^{-1} to characterize the shear thinning nature of the material which is important in order to have good printability.

3D Printing of the Silicone Ink. Direct write 3D printing was performed on a modified Alunar i3RepRap extrusion printer that has been retrofitted for pneumatic dispensation with a custom syringe holder. 3D CAD models were designed using Autodesk Fusion360 and converted to a STL file using Slicer. The objects were printed onto glass slides using a silicone ink comprised of 50:50 Dragonskin30 and Sylgard™ 184 microbeads with 0.25 weight% spiropyran. Syringes of 3cc volume were purchased from Nordson EFD and fitted with a 20-gauge polypropylene cone shaped nozzle. A pressure of 25 PSI was used to extrude the ink and the nozzle speed was set to 360 mm/s. The printed samples were cured at 85 °C for 2 h.

Results and Discussion

The development of mechanochromic silicones for direct-write 3D printing first required optimization of the silicone ink for extrusion-based processing. The ideal ink for direct-write extrusion should exhibit a yield stress and shear-thinning behavior.[35] As Sylgard™ 184 (Dow Corning) and Dragon Skin™ 30 (Smooth-On) have different Young's moduli (approximately 2050 kPa and 590 kPA, respectively)[36,37], formulations containing various combinations of beads and "bridging material" made from both precursors were tested for both the requisite properties for direct-ink extrusion and, once cured, for an extension appropriate to activate SP before material failure.[31] We further hypothesized that composites comprising beads of the stiffer Sylgard™ in the more compliant Dragon Skin™ might concentrate strain at the interface of the two components.[38] After several rounds of optimization, we arrived at a formulation of 50 wt% Sylgard™ 184 beads held together with 50 wt% Dragon Skin 30 (that displayed the requisite viscoelastic properties. The formulation exhibited a previously reported sol-gel transition,[11] indicating the formation of capillary bridges. Rheometrical characterization confirmed the

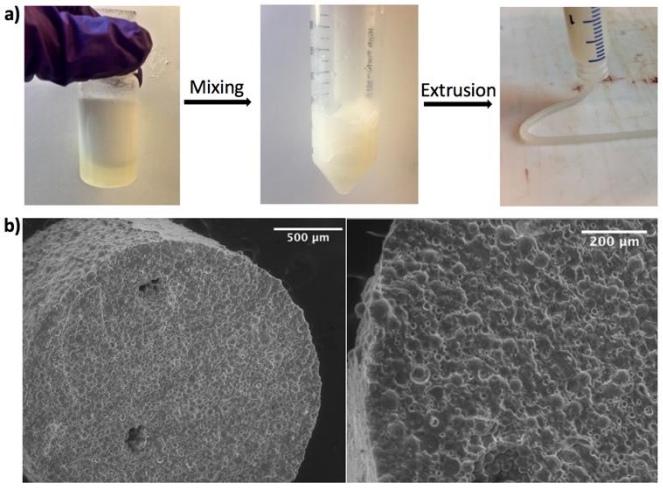

Fig. 2: a) Microbead suspension with bridging material. Upon mixing, a sol-gel transition is observed. The uncured silicone ink displayed adequate levels yield stress and shear-thinning for extrusion of multi-layered constructs. **b)** SEM images of extruded material where the **left** scale bar represents 500 μm and the **right** scale bar represents 200 μm.

yielding and shear-thinning behavior of the silicone ink (Fig. S1). The silicone ink gel exhibited a shear storage modulus on the order of 10^5 Pa that yielded at higher shear stresses. The shear-thinning nature of the material was confirmed by a decrease in viscosity of up to three orders of magnitude as a function of increasing shear rate. This allowed the formulation to be extruded from a syringe to form stable structures, which were subsequently cured (Fig. 2a). The overall formulation was rendered mechanochromic through the incorporation of 0.25 wt% SP. The SP was covalently incorporated into the PDMS network via the platinum-catalyzed hydrosilation that is responsible for the formation of cross-links in the nascent Dragon Skin 30. The cured composite displayed for SP activation, yielding reversible, visible activation by compression and tension without material failure. SEM images demonstrated the large surface area presented at the bead-matrix interfaces of the material (Fig. 2b). This interface is expected to be

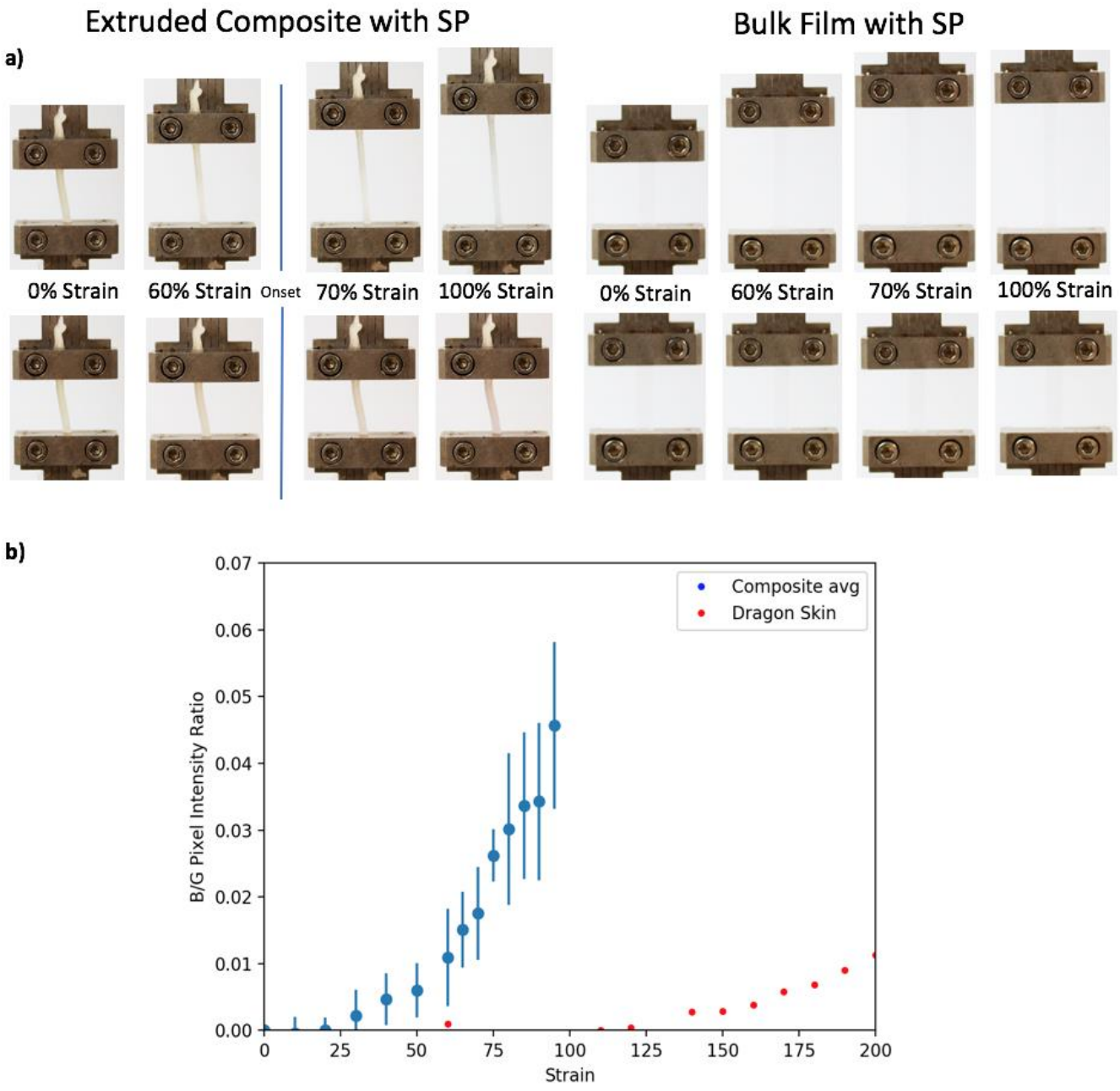

Fig. 3: a) Comparison of representative images from adapted tensile test at same strains. B/G intensity was measured from same location when the sample was returned to 0% strain. **b)** B/G values from image analysis. Extruded composite material displays mechanochromism onset between 60 and 70% strain while Dragon Skin material displays onset of similar behavior between 140 and 150% strain. Onset was determined as being greater than twice the standard deviation from the average value of B/G between 0-50% strain.

important for the increased mechanochemical activation of spiropyran.[33]

Next, we sought to evaluate the tensile strain required to activate SP in the extruded composites. The composite paste was extruded into cylindrical replicates for tensile testing that reliably achieved uniaxial strains of 100-140% before breaking. A camera was used to record the onset of color associated with SP activation during strain. To account for strain induced changes in diffraction, the ratio of the mean pixel intensity of the blue channel to that of the green channel for a small section of elastomer was employed, as reported previously.[39,40] SP isomerizes to a blue-purple MC, so the B/G channel ratio most cleanly reports mechanochromic onset. In previous reports, the onset was determined by analyzing a sequence of photographs of an ongoing tensile test that simply stretched the material until failure. The composite material is porous with numerous PDMS-to-air interfaces compared to bulk films, so light is more readily diffracted; the enhanced scattering leads to a strain-dependent background signal. To avoid complications due to the changing background, we exploited the lifetime of the MC-NO_2 derivative, which has a lifetime of several minutes after the activating force is removed.[31,38] The film was stretched cyclically with a microstrain analyzer, in a process that first took the film to a desired "activating" strain and then subsequently returned it to its zero strain resting state, at which point an image was captured (Fig. S4-S6). The use of the resting state for image acquisition minimizes the artifacts due to changes in lighting or sample geometry that might occur during stretching. The B/G pixel intensity (Fig. S7) was then analyzed at zero percent strain and recorded as a function of activating strain. As a control sample, a film of Dragon Skin 30 with 0.25 wt% SP was analyzed in the same manner to compare the onset and intensity of the mean pixel intensity ratio as a function of strain.

The threshold B/G value used as the onset of SP mechanochromism was defined to be two standard deviations beyond the mean B/G from 0-50% strain over five replicates. All composites tested displayed mechanochromic onset at B/G values corresponding to 60-75% tensile strain (Fig. 3), whereas the onset strain of mechanochromism in SP in Dragon Skin 30 is 140-150% tensile strain by the same standards. Though the composite materials displayed significantly greater B/G pixel intensity values, this is not necessarily evidence for increased percentage of mechanophore activation in the composites compared to the bulk

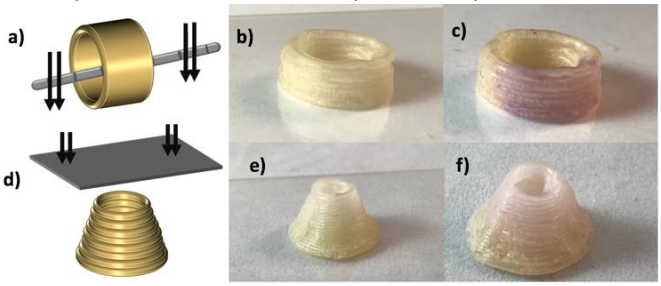

Figure 4: images showing the mechanochromic activation in 3D printed constructs : **a)** cartoon representing a hollow 3D printed cylinder with a steel rod inserted through it which was pressed on a hard surface. Images taken before **b)** and after **c)** application of force, showing a definite color change from the off-white to purple due to activation of spiropyran. **d)** Cartoon of 3D printed cone which was compressed from top with a glass slide. Images taken before **e)** and after **f)** the compression showing activation of the cured ink.

The mechanochromic silicone ink was printed using a direct-write 3D printer with pneumatic extrusion to afford the cylindrical and conical forms shown in Fig. 4. This method of printing and curing is relatively mild and is compatible with the spiropyran present in the ink formulation. The appreciable shear modulus of the gel ensured that the filament retains its tubular shape and that the multi-layered constructs held their shape until the thermal cure was completed (85 °C, overnight).

Once cured, the objects were flexible and could be stretched or compressed to activate the embedded spiropyran. Fig. 4(a) shows a cartoon depiction of a 3D printed cylinder that was pressed against a benchtop by inserting a steel rod through the central cavity, pressing down, and rolling the rod against the interior of the cylinder. A comparison of color before (Fig. 4b) and after (Fig. 4c) clearly shows the purple color associated with SP activation in the region of compression. A 3D printed cone was similarly compressed along its central axis of symmetry with a glass slide (Fig. 4d), again showing a change in color from off-white (Fig. 4e) to purple (Fig. 4f). It was observed that extent of coloration increased with the amount of pressure applied during compression (data not shown). Similar mechanochromism was observed, albeit to a lesser extent, in two dimensional auxetic meshes (Fig. S9).

Conclusions

The mechanochromic silicone inks described here provide access to mechanochemically active, 3D-printable elastomers that might be useful in expanding the many applications of PDMS-based composite materials. In addition, the PDMS-bead composite architecture provides an easily implemented strategy to improve the sensitivity of the mechanochromic response, both within and outside of the additive manufacturing space. We hypothesize that the greater sensitivity in the base material might be further enhanced in the future by utilizing 3D printed geometries that can localize the forces experienced within an object. Finally, while the mechanochromism of spiropyran is employed here as an easily characterized response, the overall strategy should be more general and could be employed to the ever-growing toolkit of mechanochemical responses available.

Conflicts of interest

There are no conflicts to declare.

Author Contributions

The experiments and data analysis for this manuscript were performed with equal contributions from R.R. and A.B. All the authors were involved in writing the manuscript. All the authors have given approval to the final version of the manuscript

Acknowledgements

This manuscript is based on work supported by the U.S. Army Research Laboratory and the Army Research Office under grant W911NF-17-1-0595 to S.L.C. and A.N. O.D.V. acknowledges support from U.S. National Science foundation award CBET-1604116. M.H.B acknowledges fellowship support from DoD

(Air Force Office of Scientific Research, NDSEG Fellowship, 32 CFR 168A to M.H.B.).

References

1 M. Hofmann, *ACS Macro Lett.*, 2014, **3**, 382–386.
2 I. T. Ozbolat and Y. Yu, *IEEE Trans. Biomed. Eng.*, 2013, **60**, 691–699.
3 L. E. Bertassoni, M. Cecconi, V. Manoharan, M. Nikkhah, J. Hjortnaes, A. L. Cristino, G. Barabaschi, D. Demarchi, M. R. Dokmeci, Y. Yang and A. Khademhosseini, *Lab Chip*, 2014, **14**, 2202–2211.
4 D.G. Yu, X.X. Shen, C. Branford-White, L. M. Zhu, K. White and X. L. Yang, *J. Pharm. Pharmacol.*, 2009, **61**, 323–329.
5 C. Zhao, C. Wang, R. Gorkin, S. Beirne, K. Shu and G. G. Wallace, *Electrochem. commun.*, 2014, **41**, 20–23.
6 G. M. Gratson, M. Xu and J. A. Lewis, *Nature*, 2004, **428**, 386.
7 C. Ladd, J. H. So, J. Muth and M. D. Dickey, *Adv. Mater.*, 2013, **25**, 5081–5085.
8 S. Roh and O. D. Velev, *AIChE J.*, 2018, **64**, 3558–3564.
9 S. Zheng, M. Zlatin, P. R. Selvaganapathy and M. A. Brook, *Addit. Manuf.*, 2018, **24**, 86–92.
10 Z. Qin, B. G. Compton, J. A. Lewis and M. J. Buehler, *Nat. Commun.*, 2015, **6**, 7038.
11 S. Roh, D. P. Parekh, B. Bharti, S. D. Stoyanov and O. D. Velev, *Adv. Mater.*, 2017, **29**, 1701554.
12 S. Roh, L. B. Okello, N. Golbasi, J. P. Hankwitz, J. A.-C. Liu, J. B. Tracy and O. D. Velev, *Adv. Mater. Technol.*, 2019, **4**, 1800528.
13 A. J. Boydston, B. Cao, A. Nelson, R. J. Ono, A. Saha, J. J. Schwartz and C. J. Thrasher, *J. Mater. Chem. A*, 2018, **6**, 20621–20645.
14 J. Raasch, M. Ivey, D. Aldrich, D. S. Nobes and C. Ayranci, *Addit. Manuf.*, 2015, **8**, 132–141.
15 F. S. Senatov, K. V Niaza, M. Y. Zadorozhnyy, A. V Maksimkin, S. D. Kaloshkin and Y. Z. Estrin, *J. Mech. Behav. Biomed. Mater.*, 2016, **57**, 139–148.
16 M. Zarek, M. Layani, I. Cooperstein, E. Sachyani, D. Cohn and S. Magdassi, *Adv. Mater.*, 2016, **28**, 4449–4454.
17 Y. L. Kong, I. A. Tamargo, H. Kim, B. N. Johnson, M. K. Gupta, T. W. Koh, H. A. Chin, D. A. Steingart, B. P. Rand and M. C. McAlpine, *Nano Lett.*, 2014, **14**, 7017–7023.
18 J. H. Kim, W. S. Chang, D. Kim, J. R. Yang, J. T. Han, G.-W. Lee, J. T. Kim and S. K. Seol, *Adv. Mater.*, 2015, **27**, 157–161.
19 C. A. Mandon, L. J. Blum and C. A. Marquette, *Anal. Chem.*, 2016, **88**, 10767–10772.
20 A. Kirillova, R. Maxson, G. Stoychev, C. T. Gomillion and L. Ionov, *Adv. Mater.*, 2017, **29**, 1703443.
21 G. I. Peterson, M. B. Larsen, M. A. Ganter, D. W. Storti and A. J. Boydston, *ACS Appl. Mater. Interfaces*, 2015, **7**, 577–583.
22 B. Cao, N. Boechler and A. J. Boydston, *Polymer*, 2018, **152**, 4–8.
23 H. Staudinger and H. F. Bondy, *Berichte der Dtsch. Chem. Gesellschaft.*, 1930, **63**, 734–736.
24 J. Li, C. Nagamani and J. S. Moore, *Acc. Chem. Res.*, 2015, **48**, 2181–2190.
25 T. Matsuda, R. Kawakami, R. Namba, T. Nakajima and J. P. Gong, *Science*, 2019, **363**, 504 LP – 508.
26 T. Shiraki, C. E. Diesendruck and J. S. Moore, *Faraday Discuss.*, 2014, **170**, 385–394.
27 D. A. Davis, A. Hamilton, J. Yang, L. D. Cremar, D. Van Gough, S. L. Potisek, M. T. Ong, P. V Braun, T. J. Martínez, S. R. White, J. S. Moore and N. R. Sottos, *Nature*, 2009, **459**, 68.
28 Y. Sagara, M. Karman, E. Verde-Sesto, K. Matsuo, Y. Kim, N. Tamaoki and C. Weder, *J. Am. Chem. Soc.*, 2018, **140**, 1584–1587.
29 G. R. Gossweiler, T. B. Kouznetsova and S. L. Craig, *J. Am. Chem. Soc.*, 2015, **137**, 6148–6151.
30 A. L. B. Ramirez, A. K. Schmitt, M. K. Mahanthappa and S. L. Craig, *Faraday Discuss.*, 2014, **170**, 337–344.
31 G. R. Gossweiler, G. B. Hewage, G. Soriano, Q. Wang, G. W. Welshofer, X. Zhao and S. L. Craig, *ACS Macro Lett.*, 2014, **3**, 216–219.
32 K. S. Suslick, *Faraday Discuss.*, 2014, **170**, 411–422.
33 J. Frenkel, *Acta Physiochim*, 1944, **19**, 51–76.
34 J. Li, T. Shiraki, B. Hu, R. A. E. Wright, B. Zhao and J. S. Moore, *J. Am. Chem. Soc.*, 2014, **136**, 15925–15928.
35 P. T. Smith, A. Basu, A. Saha and A. Nelson, *Polymer,* 2014 **152**, 42-50
36 I. D. Johnston, D. K. McCluskey, C. K. L. Tan and M. C. Tracey, *J. Micromech. Microeng.,* 2014, **24**, 35017
37 Dragon Skin™ Series Mechanical Properties, https://www.smooth-on.com/tb/files/DRAGON_SKIN_SERIES_TB.pdf (accessed August 2019)
38 S. Park, K. Mondal, R. M. Treadway, V. Kumar, S. Ma, J. D. Holbery and M. D. Dickey, *ACS Appl. Mater. Interfaces*, 2018, **10**, 11261–11268.
39 M. H. Barbee, K. Mondal, J. Z. Deng, V. Bharambe, T. V Neumann, J. J. Adams, N. Boechler, M. D. Dickey and S. L. Craig, *ACS Appl. Mater. Interfaces*, 2018, **10**, 29918–29924.
40 G. R. Gossweiler, C. L. Brown, G. B. Hewage, E. Sapiro-Gheiler, W. J. Trautman, G. W. Welshofer and S. L. Craig, *ACS Appl. Mater. Interfaces*, 2015, **7**, 22431–22435.

Composite silicone inks provide access to 3D-printable elastomers that are mechanochemically active at lower strains that single component analogs.